Modeling of global biogenic emissions for key indirect greenhouse gases and their response to atmospheric CO_2 increases and changes in land cover and climate

Zhining Tao and Atul K. Jain
Department of Atmospheric Science, University of Illinois, Urbana, Illinois, USA

Received 11 February 2005; revised 2 June 2005; accepted 27 July 2005; published 10 November 2005.

[1] Natural emissions of nonmethane volatile organic compounds (NMVOCs) play a crucial role in the oxidation capacity of the lower atmosphere and changes in concentrations of major greenhouse gases (GHGs), particularly methane and tropospheric ozone. In this study, we integrate a global biogenic model within a terrestrial ecosystem model to investigate the vegetation and soil emissions of key indirect GHGs, e.g., isoprene, monoterpene, other NMVOCs (OVOC), CO, and NOx. The combination of a high-resolution terrestrial ecosystem model with satellite data allows investigation of the potential changes in net primary productivity (NPP) and resultant biogenic emissions of indirect GHGs due to atmospheric CO_2 increases and changes in climate and land use practices. Estimated global total annual vegetation emissions for isoprene, monoterpene, OVOC, and CO are 601, 103, 102, and 73 Tg C, respectively. Estimated NOx emissions from soils are 7.51 Tg N. The land cover changes for croplands generally lead to a decline of vegetation emissions for isoprene OVOC, whereas temperature and atmospheric CO_2 increases lead to higher vegetation emissions. The modeled global mean isoprene emissions show relatively large seasonal variations over the previous 20 years from 1981 to 2000 (as much as 31% from year to year). Savanna and boreal forests show large seasonal variations, whereas tropical forests with high plant productivity throughout the year show small seasonal variations. Results of biogenic emissions from 1981 to 2000 indicate that the CO_2 fertilization effect, along with changes in climate and land use, causes the overall up-trend in isoprene and OVOC emissions over the past 2 decades. This relationship suggests that future emission scenario estimations for NMVOCs should account for effects of CO_2 and climate in order to more accurately estimate local, regional, and global chemical composition of the atmosphere, the global carbon budget, and radiation balance of the Earth-atmosphere system.

Citation: Tao, Z., and A. K. Jain (2005), Modeling of global biogenic emissions for key indirect greenhouse gases and their response to atmospheric CO_2 increases and changes in land cover and climate, *J. Geophys. Res.*, *110*, D21309, doi:10.1029/2005JD005874.

1. Introduction

[2] It is well documented that indirect greenhouse gases (GHGs), e.g., nonmethane volatile organic compounds (NMVOCs), carbon monoxide (CO), and nitric oxides (NOx), can impact the climate system by altering concentrations of methane (CH_4) and tropospheric ozone (O_3), two important GHGs [*Fuglestvedt et al.*, 1996; *Daniel and Solomon*, 1998; *Kheshgi et al.*, 1999; *Kheshgi and Jain*, 1999; *Hayhoe et al.*, 2000]. The NMVOCs also play an important role in the global carbon budget [*Guenther*, 2002] and radiation balance of the Earth-atmosphere system [*Otter et al.*, 2003]. Terrestrial vegetation remains a major source of indirect GHGs, particularly for NMVOCs, on a global scale [*Intergovernmental Panel on Climate Change* (*IPCC*), 2001]. Moreover, emissions of indirect GHGs are highly dependent on environmental conditions, such as temperature, solar radiation, atmospheric CO_2 concentration, and the resultant foliar density [e.g., *Guenther et al.*, 1995], and nonenvironmental factors, such as changes in land cover [*Purves et al.*, 2004].

[3] Foliage (leaves and needles) is the primary source of isoprene, monoterpene, and other NMVOC (OVOC) emissions, though the emission mechanism for each species is different [*Fall*, 1999; *Kesselmeier and Staudt*, 1999; *Guenther et al.*, 2000; *Guenther*, 2002]. Isoprene, with the largest biogenic emission rate, is not stored in plant tissues but rather is produced in plant chloroplasts through photosynthesis [*Silver and Fall*, 1995]. Its emissions peak during the daytime when the photosynthetically active radiation (PAR) reaches maximum, and then reduce to zero during the nighttime. Isoprene emissions are primarily controlled by leaf temperature, PAR, and leaf age. Monoterpene, on the other hand, is stored in plant reservoirs and emitted from specialized plant tissues throughout the day and night [*Fall*,

0148-0227/05/2005JD005874$09.00

1999]. Although leaf temperature is mainly responsible for the magnitude of monoterpene emissions, studies suggest that monoterpene emissions from some plant species are light-dependent [*Bertin et al.*, 1997; *Kesselmeier and Staudt*, 1999; *Owen et al.*, 2002]. More monoterpene is generally emitted at higher temperatures. The mechanism of OVOC emissions varies with different OVOC species and is summarized by *Guenther* [2002].

[4] In the case of CO, laboratory studies suggest that it is emitted from live leaves as the result of a direct photochemical transformation of leaf matter on or in the plant matrix [*Tarr et al.*, 1995]. The dead plant matter also emits CO as a result of photo-oxidation of plant cellular materials from ultraviolet (UV) solar radiation. On the basis of laboratory and field measurements, *Schade et al.* [1999] found that not only did solar radiation contribute to plant CO production, but also temperature played an important role. The NOx (in the form of NO) is emitted from biogenic sources as the result of biological nitrification and denitrification [e.g., *Potter et al.*, 1996]. Many factors, like soil nitrogen availability, soil temperature, and soil water content, regulate soil NO emissions [e.g., *Galbally and Roy*, 1978; *Yienger and Levy*, 1995].

[5] There are a number of studies of total NMVOC emissions on a regional and global scale [e.g., *Geron et al.*, 1994; *Guenther et al.*, 1995, 1999, 2000; *Simpson et al.*, 1995; *Wang and Shallcross*, 2000; *Adams et al.*, 2001; *Potter et al.*, 2001; *Levis et al.*, 2003; *Otter et al.*, 2003; *Stewart et al.*, 2003; *Tao et al.*, 2003; *Naik et al.*, 2004]. Most of these studies have applied *Guenther et al.'s* [1995] algorithm to calculate NMVOC emissions. The differences are generally in the details of input data for the globe or specific regions. For example, *Guenther et al.* [1995] estimated the global natural VOC emissions using a high-resolution emission model. They applied the emission rates (μg C g^{-1} dry foliar mass h^{-1}) of isoprene, monoterpene, and OVOC to individual ecosystem type, and modified the emissions using environmental correction factors that accounted for leaf temperature and PAR. *Guenther et al.* [1999, 2000] further revised the isoprene emission algorithm by adding a so-called "leaf age" factor. More recently, *Stewart et al.* [2003] applied Guenther's algorithm to calculate the biogenic isoprene and monoterpene emissions across Great Britain with very detailed plant-specific land use and meteorology.

[6] Unlike vegetation NMVOC emissions, there are very few studies available in the literature on biogenic emissions of CO and NO. *Schade and Crutzen* [1999] developed a model to calculate the global vegetation CO emissions. They estimated global vegetation emissions from photochemical degradation of plant matter and thermal CO production. More recently, *Guenther et al.* [2000] calculated the vegetation CO emissions from North America using an emission factor method. In the case of NO, *Williams et al.* [1992] developed an algorithm that combined biome type and soil temperature to calculate soil NO emissions for the US, which was later applied to calculate NO emissions for Europe [*Stohl et al.*, 1996], and for the globe [*Lee et al.*, 1997]. *Yienger and Levy* [1995] also developed an algorithm to estimate the global soil NO emissions, which accounted for details such as "pulsing," nitrogen fertilizer stimulation, biomass burning stimulation, and canopy reduction. *Potter et al.* [1996] employed a process-based ecosystem model in combination with nitrogen mineralization rates and soil inundation to calculate global soil emissions of NO.

[7] The purpose of this study is to build on and extend the approaches of previous studies. While we use the same or similar algorithms to calculate biogenic emissions for indirect GHGs, we implement these algorithms in the newly developed terrestrial ecosystem model component [*Jain and Yang*, 2005] of the Integrated Science Assessment Model (ISAM) to estimate the emissions of indirect GHGs from biogenic sources. The advantage of implementing the biogenic emission relationship into the ISAM terrestrial ecosystem model is to provide the capability of investigating potential time-dependent changes in biogenic emissions due to changes in ecological and physiological processes, and their interactions with atmospheric CO_2, climate, and land cover change practices. We would like to mention here that two recent global modeling studies have investigated the effects of climate variations and increasing atmospheric CO_2 on global NMVOC emissions [*Levis et al.*, 2003; *Naik et al.*, 2004]. *Levis et al.* [2003] calculated the terrestrial biogenic volatile organic compound emissions using CCSM's (Community Climate System Model's) dynamic vegetation model [*Bonan et al.*, 2002], whereas *Naik et al.* [2004] estimated emissions using the Integrated Biospheric Simulators (IBIS2.5) [*Foley et al.*, 1996]. Both modeling frameworks incorporated the *Guenther et al.* [1995] vegetation emissions algorithms to account for the influence of temperature and radiation on emissions. However, to our knowledge, no published work has been done to study the effect of human land cover changes on the indirect GHGs. Therefore, as an extension of previous studies, the objectives of the current study are two fold. First, we estimate spatial and temporal biogenic emissions of the indirect GHGs (isoprene, monoterpene, OVOC, CO, and NOx) over the globe for the current atmospheric composition using ISAM. Secondly, we estimate the historical seasonal variations in biogenic emissions of the indirect GHGs over the past 20 years from 1981 to 2000 due to changes in atmospheric CO_2, climate, and changes in land use. These emissions could be used to study the past climate variability.

2. Method

[8] The algorithm of biogenic emissions is linked to the terrestrial ecosystem component of the ISAM [*Jain and Yang*, 2005]. The terrestrial model is used to calculate net primary productivity (*NPP*) that drives the estimate of foliar density. Biogenic emissions are calculated by multiplying a prescribed emission factor by foliar density, an environmental adjustment factor that accounts for the influence of photosynthetic photon flux density (PPFD), temperature, and leaf age, and an escape efficiency that represents the fraction that is released into the above-canopy atmosphere. The ground-based gridded monthly temperature and precipitation data ($0.5^\circ \times 0.5^\circ$ resolution) are from T. D. Mitchell et al. (A comprehensive set of high-resolution grids of monthly climate for Europe and the globe: The observed record (1901–2000) and 16 scenarios (2001–2100), submitted to *Journal of Climate*, 2003, hereinafter referred to as Mitchell et al., submitted manuscript, 2003). The gridded

Table 1. Emission Factors for Indirect GHGs and Empirical Parameters for Each Biome Type Used in This Study[a]

Biome Type	Emission Factors, ug C g^{-1} dry foliar mass h^{-1}						
	Isoprene[b]	Monoterpene[b]	OVOC[b]	CO[c]	A,[d] ug N m^{-2} h^{-1}, NOx	D_r[e]	CRF[f]
Tropical evergreen	0.7–18.1	0.13–0.70	0.13–0.41	0.3	9.13	0.55	0.78
Tropical deciduous	0.8–10.9	0.20–0.91	0.20–0.56	0.3	3.60	0.55	0.55
Temperate evergreen	0.1–45.0	0.09–1.42	0.21–0.68	0.3	0.252	0.45	0.55
Temperate deciduous	1.5–147.5	0.28–22.5	0.47–12.9	0.3	0.252	0.35	0.48
Boreal	0.2–80.0	0.15–7.43	0.15–4.39	0.3	0.252	1.30	0.50
Savanna	0.4–75.0	0.08–1.23	0.08–0.63	0.3	3.24	0.50	0.30
Grassland	~0.	~0.10	0.32–3.06	0.3	3.24	0.50	0.28
Shrubland	0.2–90.0	0.05–4.25	0.06–2.24	0.3	1.746	0.45	0.30
Tundra	1.5–10.0	0.09–1.25	0.11–0.62	0.3	~0.	0.50	0.21
Desert	0.7–20.0	0.18–1.60	0.21–0.85	0.3	0.252	0.30	0.20
Polar desert/rock/ice	~0.	~0.	~0.	0.3	~0.	0.30	0.20
Cropland	~0.	0.06–0.10	0.09–4.99	0.3	see text	0.75	0.32
Pasture	~0.	0.08–0.10	0.10–4.02	0.3	3.24	0.50	0.30

[a]Emission factors for isoprene, monoterpene, and OVOC are gridded based and the range of values for each biome type is provided.
[b]Guenther et al. (manuscript in preparation, 2005).
[c]*Guenther et al.* [2000] and *Levis et al.* [2003].
[d]*Williams et al.* [1992].
[e]*Guenther et al.* [1995].
[f]Average of *Yienger and Levy* [1995] and *Lee et al.* [1997].

surface shortwave solar radiation data are from the Earth Radiation Budget Experiment (ERBE) database (2.5° × 2.5° resolution) [*Li and Leighton*, 1993; *Li et al.*, 1993]. The gridded monthly leaf area index (LAI) data are from the NASA MODIS Land Discipline data set [*Myneni et al.*, 1997; http://cliveg.bu.edu/modismisr/products/avhrr/avhrrlaifpar.html].

2.1. Terrestrial Ecosystem Component of ISAM

[9] In this study the global and annual *NPP* is calculated using the terrestrial component of our ISAM, which simulates carbon fluxes to and from different compartments of the terrestrial biosphere with 0.5° × 0.5° spatial resolution [*Jain and Yang*, 2005]. Each grid cell is completely occupied by at least one of the 13 land coverage classifications (Table 1). The global distributions for different land cover classifications are primarily based on *Loveland and Belward* [1997] and *Haxeltine and Prentice* [1996] vegetation data sets. Each grid is also assigned one of the 105 soil types on the basis of the FAO-UNESCO Soil Map of the World [*Zobler*, 1986, 1999]. Within each grid cell, the carbon dynamics of each land coverage classification are described by an ecosystem model, which consists of three vegetation carbon reservoirs (ground vegetation (GV), nonwoody tree part (NWT), and woody tree part (WT)); two litter reservoirs (DPM and RPM) representing above and below ground litter biomass; and three soil reservoirs (microbial biomass (BIO), humified organic matter (HUM), and inert organic matter (IOM)). We calculate actual soil water (mm) and soil water pressure (kPa) for each grid cell with the monthly climatic water budget model of *Thornthwaite and Mather* [1957] as implemented by *Pastor and Post* [1985]. The soil hydraulic characteristics for the soil moisture function and the water balance calculations are derived from soil depth and texture information for each FAO soil type [*Zobler*, 1986, 1999], rooting depth estimates [*Webb et al.*, 1991], and relationships between soil texture and water content at the critical pressure [*Rawls et al.*, 1982]. Within each grid cell, the model simulates the processes of evapotranspiration, plant photosynthesis and respiration, carbon allocation among plant organs, litter production, and soil organic carbon decomposition. The model also includes effects of biomass regrowth in response to feedback processes such as CO_2 fertilization and temperature effects on photosynthesis and respiration. Plant and soil carbon stocks for land coverage classifications are also influenced by agriculture, forest, and nonforest change cover activities [*Jain and Yang*, 2005].

[10] Because of the long turnover times of some model reservoirs, the carbon is accumulated over many years to generate the biomass in different terrestrial ecosystem reservoirs. Therefore we first initialized the vegetation model with a 1765 atmospheric CO_2 concentration of 278 ppmv to calculate the equilibrium *NPP* in addition to vegetation and soil carbon for different model pools. Next, we ran the model up to the year 2000 using prescribed observed temperature and precipitation changes (Mitchell et al., submitted manuscript, 2003) and CO_2 concentrations [*Neftel et al.*, 1985; *Friedli et al.*, 1986; *Keeling and Whorf*, 2000]. We also utilized surveys of past land cover changes due to three types of land cover change activities: clearing of natural ecosystems for croplands and pasturelands, recovery of abundant croplands/pasturelands to preconversion natural vegetation, and production and harvest in conversion areas [*Jain and Yang*, 2005]. For the land cover changes we employed the *Ramankutty and Foley* [1998, 1999] data set, which was available for the period 1765–1992. Between 1992 and 2000, we linearly extrapolated each grid cell data using the trend for the 1980s. The *Ramankutty and Foley* [1998, 1999] data set was derived from spatially explicit maps of historical land use changes using a satellite based 1992 cropland data [*Haxeltine and Prentice*, 1996; *Loveland and Belward*, 1997] and historical inventory data compiled from various sources [*Ramankutty and Foley*, 1998, 1999]. The estimates represent the extent to which different natural vegetation types have been changed, and which have been abandoned over the historical time period. We do not explicitly account for land cover changes due to succession and species composition over time. These changes are implicitly accounted for the inven-

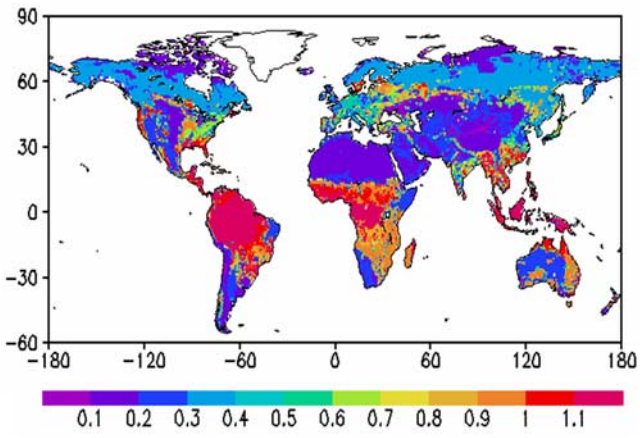

Figure 1. ISAM estimated net primary productivity (*NPP*, kg C m^{-2} yr^{-1}) for the year 2000.

tory data. The changes in carbon stock due to land cover change activities are calculated using a land use change model [*Jain and Yang*, 2005]. In this model, changes in carbon stocks following the land cover changes are affected by the changes in *NPP* and soil respiration, and the effects of changing environmental conditions on these fluxes. This modeling approach allows us to study the concurrent effects of time-dependent variations in CO_2, climate, and land cover change activities on biogenic emissions of indirect GHGs.

[11] Figure 1 shows the ISAM estimated annual mean global distribution of *NPP* for the year 2000. Modeled global *NPP* for 2000 is about 63 Gt C (10^9 tons of carbon), a magnitude similar to other global estimates [*Prentice et al.*, 2001, and references therein]. Tropical evergreen forests account for about 22% of the total *NPP*, followed by savanna (~15%), cropland (~13%), and boreal forests (~10%). The remaining 40% of *NPP* is distributed among the other 9 biomes. As noted by *Jain and Yang* [2005], the model estimated *NPPs* are consistent with other estimates [*Cramer et al.*, 1999; *Prentice et al.*, 2001].

2.2. Biogenic Emission Component of ISAM

2.2.1. Vegetation VOC and CO Emissions

[12] Trace gas emissions from vegetation (E, μg C h^{-1}) are estimated as [*Guenther et al.*, 1995, 1999, 2000]:

$$E = \varepsilon \times D \times \gamma \times \rho \times A \quad (1)$$

where ε is a gridded emission factor (μg C g^{-1} dry foliar mass h^{-1}), D is the monthly foliar density (dry foliar mass m^{-2}), γ is the environmental adjustment factor, ρ is the escape efficiency that represents the fraction of emissions entering the above-canopy atmosphere, and A denotes the ground vegetation area of the grid cell of the respective biome type (m^2).

2.2.1.1. Emission Factors (ε)

[13] There have been a number of measurements of ε for a wide range of plant species over the globe [e.g., *Janson*, 1993; *Guenther et al.*, 1996a, 1996b; *Ciccioli et al.*, 1997; *Geron et al.*, 1997, 2002; *Steinbrecher et al.*, 1997; *Hakola et al.*, 1998; *Greenberg et al.*, 1999; *Helmig et al.*, 1999; *Pattey et al.*, 1999; *Harley et al.*, 2003]. Since our terrestrial model cannot explicitly represent such a wide variety of plant species, we do not assign ε on a biome basis. Instead, each model grid cell was assigned weighted average ε on the basis of global measurement data of six plant functional types (PFTs): broadleaf trees, fine-leaf evergreen trees, fine-leaf deciduous trees, shrubs, grass, and crops, based on measurements. The weighted average ε are calculated on the basis of the area fraction of each PFT within each grid cell, and are available for isoprene, monoterpene and OVOC from a public access database developed by Alex Guenther and colleagues (https://cdp.ucar.edu/.) (A. Guenther et al., Emissions of gases and aerosols from Nature, manuscript in preparation, 2005, hereinafter referred to as Guenther et al., manuscript in preparation, 2005).

[14] The advantage of using the gridded ε is that it reduces the uncertainty due to large variations in ε within the same biome type classified by the terrestrial model. Table 1 lists the ε ranges of isoprene, monoterpene, and OVOC for each biome type defined in our terrestrial model, which are assemblies of area weighted ε. As these figures illustrate, the ε for NMVOCs vary widely, mainly because there are large regional differences in the ε for the same biome type as biomes in different climates respond very differently. The ε for OVOC represent all the NMVOCs other than isoprene and monoterpene, including recently documented high vegetation emissions of methanol [*Heikes et al.*, 2003] and acetone [*Potter et al.*, 2003]. The ε for CO is from *Guenther et al.* [2000] and *Levis et al.* [2003], and can only be regarded as a rough estimate because of the lack of data.

2.2.1.2. Foliar Density (D)

[15] The monthly foliar density (D) is estimated from *Guenther et al.* [1999, 2000]:

$$D = D_f \times D_p \quad (2)$$

where D_f is the ratio of the monthly LAI to the peak LAI [*Guenther et al.*, 2000]. D_p is calculated on the basis of *Guenther et al.* [1995]:

$$D_p = D_r \times NPP \quad (3)$$

where D_r is a biome type–dependent empirical coefficient, which is obtained from *Guenther et al.* [1995] and listed in Table 1. The annual *NPP* is calculated using the terrestrial ecosystem component of the ISAM, which has been discussed in section 2.1.

2.2.1.3. Environmental Adjustment Factor (γ)

[16] The environmental adjustment factor is estimated in a different manner for different gases. Isoprene emissions are strongly controlled by leaf temperature and solar radiation [*Guenther et al.*, 1993, 1995; *Geron et al.*, 1994], as well as leaf age [*Guenther et al.*, 1999]. Therefore γ for isoprene is calculated by taking into account these factors:

$$\gamma_{iso} = \gamma_T \times \gamma_L \times \gamma_A \quad (4)$$

where γ_T, γ_L, and γ_A are the environmental adjustment factors due to leaf temperature, solar radiation, and leaf age, respectively. Estimations of γ_T and γ_L are made using the empirical equations by *Guenther et al.* [1993]. γ_A is

estimated with the method employed by *Guenther et al.* [1999].

[17] The empirical equation developed by *Guenther et al.* [1993], which is a function of temperature, is used to calculate γ for individual vegetation emissions of monoterpene, OVOC, and CO:

$$\gamma_{Others} = \exp[\beta \times (T - T_S)] \quad (5)$$

where β (=0.09 K^{-1}) is an empirical coefficient, T_S denotes the standard temperature (=303 K); T is the leaf temperature. Here we use the surface skin temperatures to represent leaf temperatures as applied and cautioned by *Pierce et al.* [1998]. Radiation profiles within the canopy are estimated using the method employed in USEPA's SMOKE model [*Houyoux et al.*, 2000].

2.2.1.4. Escape Efficiency (ρ)

[18] Escape efficiency is a function of deposition and canopy ventilation rates and can be estimated using the model by *Jacob and Bakwin* [1991]. In this study, we did not explicitly estimate ρ, but rather we applied the ρ values derived by *Guenther et al.* [1999, 2000] for our calculation.

2.2.2. NOx Emissions From Soils

[19] Soil type and temperature are key factors in the determination of NOx emissions from soils. Leaf uptake and deposition are also significant because they reduce the amount of NO_2 released into the free troposphere. To calculate soil biogenic NOx emissions, we use soil temperature-dependent semiempirical algorithm based on *Williams et al.* [1992] but with additions to explicitly account for the "pulsing," canopy reduction and linear dependence of fertilization rates:

$$E = A \times \gamma_{NO} \times (1 - CRF) \times Area \times PL \quad (6)$$

$$\gamma_{NO} = \exp(\theta \times T_{soil}) \quad (7)$$

where A (μg N m^{-2} h^{-1}) is similar to a emission factors (ε) and reflects the physical and chemical properties of soils, such as soil nutrient and water content. Unlike grid-based ε for NMVOCs, here we use biome-dependent A factor because of lack of observations for all the specific soil types considered in this study. Except for the agriculture biome, the A factors chosen for this study are primarily based on *Williams et al.* [1992] (Table 1). The A factor for the agriculture biome is calculated on the basis of the approach of *Yienger and Levy* [1995], which makes A factor for crop biome linearly dependent on the N fertilizer rate and constrain it to force a 2.5% loss of N fertilizer annually per grid [*Yienger and Levy*, 1995]. θ (=0.071 $\pm$ 0.007 $°C^{-1}$) is an empirical coefficient. The monthly fertilizer rates are derived from FAO country-specific annual fertilization use [*International Fertilizer Industry Association*, 2005], which we uniformly distribute over the growing period. T_{soil} denotes soil temperature (°C). Here we use the algorithms by *Houyoux et al.* [2000] to convert air temperature to soil temperature for different biome types. *CRF* is the biome-dependent canopy reduction factor, representing NO_2 loss before escaping the plant canopy. The NO_2 is lost because of diffusion through plant stomata, direct deposition of NO_2 onto and through the cuticle, and deposition of NO_2 onto surface soils [*Yienger and Levy*, 1995; *Ganzeveld et al.*, 2002]. In equation (6), (1 − *CRF*) term represents the amount of NOx released above canopy. The *CRF* values are taken from *Yienger and Levy* [1995] (Table 1), which are calculated from the amount of biomass, expressed by the leaf area index, and the stomatal area index to represent the uptake of NO_2 by the leaf cuticle and stomata. The applicability of the *CRF* is confirmed by the study of *Ganzeveld et al.* [2002] that employs a multilayer canopy model to study the effect of *CRF* on NOx emissions. *PL* is the pulsing term, which accounts for large burst of emissions of NO after a very dry soil is wetted because of rainfall. We applied *Yienger and Levy* [1995] algorithm to estimate the pulsing effect, which was a function of rainfall intensity. We used the model estimated soil moisture to distinguish between dry and wet soil.

2.3. Model Experiments

[20] Studies suggest that a number of environmental factors, including temperature, radiation, CO_2 increase, water availability, and land use changes could be playing significant roles in the biogenic emissions [*Fuentes et al.*, 2001]. It is conceivable that their combined effect could counterbalance to each other. For example, historical deforestation rates must have produced a decrease in emissions rates, whereas abandonment of agriculture and subsequent forest management must have increased the emissions. *NPP* may increase because of climate and CO_2 fertilization-enhanced productivity of plants, whereas *NPP* may reduce because of climate change–increased autotrophic respirations. There may also be strong interactions between the regrowth component and the other mechanisms. For example, the effect of increasing CO_2 in forests may be strongest during rapid regrowth leading to faster canopy development and higher photosynthesis. Thus the overall terrestrial carbon balance may differ between analyses that do not simultaneously consider the major factors influencing changes in biogenic emissions of NMVOCs. To assess the concurrent effects of land cover changes, CO_2 concentrations, and climate change on spatial and monthly mean biogenic emissions of NMVOCs over the past 2 decades (1981–2000), we performed four experiments using our ISAM terrestrial modeling framework. In the first experiment, *E1*, land cover changes, atmospheric CO_2, and climate were varied over the period 1981–2000. In the second experiment, *E2*, land cover, atmospheric CO_2, and climate remained constant at the 1980 level. In experiment *E3*, only atmospheric CO_2 and climate were varied with time. In the final experiment, *E4*, only land cover changes and atmospheric CO_2 were varied. The impact of land cover changes was estimated by subtracting *E3* from *E1*, and the effect of climate changes was obtained by subtracting *E4* from *E1*. The marginal effect of increasing CO_2 was determined by subtracting *E2*, the land use and climate change effects from *E1*. The isoprene emissions were used in this study to illustrate the model results.

3. Results and Discussion

3.1. Base Year Simulation

[21] We select year 2000 as our base simulation year to which our model results would be compared. The ISAM

Table 2. Estimated Annual Biogenic Emissions of Indirect GHGs From Each Biome in 2000

Biome	Isoprene, Tg C	Monoterpene, Tg C	OVOC, Tg C	CO, Tg C	NOx, Tg N		
					With CRF	No "Pulsing"	No CRF
Tropical evergreen	217.2	41.4	33.9	31.7	1.415	0.934	6.432
Tropical deciduous	28.3	5.9	4.7	3.6	0.201	0.153	0.444
Temperate evergreen	11.3	4.5	2.6	1.8	0.007	0.005	0.017
Temperate deciduous	7.0	2.1	1.7	0.5	0.005	0.003	0.011
Boreal	20.6	12.7	7.8	4.8	0.025	0.020	0.049
Savanna	130.9	17.7	14.9	13.0	1.126	0.898	1.607
Grassland	0.	0.5	6.7	1.4	0.599	0.534	0.832
Shrubland	167.0	12.3	12.1	4.0	0.613	0.566	0.878
Tundra	0.8	0.5	0.3	0.1	0.	0.	0.
Desert	17.9	2.3	2.1	1.9	0.024	0.024	0.035
Polar desert/rock/ice	0.	0.	0.	0.	0.	0.	0.
Cropland	0.	3.3	11.8	9.8	3.006	2.448	4.419
Pasture	0.	0.2	3.4	0.6	0.488	0.391	0.697
Total	601.0	103.4	102.0	73.2	7.509	5.976	15.42

estimated global and annual total vegetation emissions based on the *E1* experiment for the year 2000 are 601 Tg C of isoprene, 103 Tg C of monoterpene, 102 Tg C of OVOC, and 73 Tg C of CO (Table 2). The estimated NOx emissions from soils associated with and without the *CRF* effects are approximately 7.5 and 15.4 Tg N (Table 2), respectively. Although tropical evergreen forests occupy approximately 11% of the total global land area, they account for more than 36% of total isoprene emissions. Shrubland and savanna rank 2nd and 3rd in isoprene emissions, accounting for 28% and 22%, respectively. Forests and savanna are also big contributors to vegetation emissions of monoterpene, OVOC, and CO, accounting for 82%, 64%, and 76% of the total emissions, respectively. On a global scale, croplands emit about 40% of the total NOx from soils when the *CRF* effect is considered, followed by tropical evergreen forests (19%) and savanna (15%). Shrubland, grassland, and pastureland account almost 90% of the remaining 26% of NOx emissions from soils. It should be noted that more than 2 Tg N of the 3 Tg N emitted from croplands are induced by the application of N-containing fertilizer (Table 3). Pulsing effect accounts for 1.53 Tg N or 20% of total (7.51 Tg N) soil emissions. Approximately 70% of the total pulsing effect comes from tropical regions (Table 2). Without the *CRF*, however, emissions from tropical evergreen forest increase by a factor of 4 and account for approximately 42% of the total NOx emissions. In that case, the cropland emissions reduce to 29%, and become the second highest contributor to NOx emissions from soils.

[22] Figure 2 displays the latitudinal variations in relative contributions to the global biogenic emissions of indirect GHGs. There are two peaks of isoprene emissions, centering on the equator and 24°S, respectively. Heavy biomass, high temperature, and strong solar radiation are responsible for intense emissions there. Vegetation emissions of monoterpene, OVOC, and CO have similar global latitudinal patterns driven by variations in biomass and temperature. In general, vegetation emissions peak along the equator and decrease poleward. Tropical (30°S to 30°N) emissions are approximately 89%, 78%, 77%, and 85% of global emissions of isoprene, monoterpene, OVOC, and CO, respectively. Another peak is centered on 60°N for monoterpene emissions. Boreal forests are the major contributor to this other peak. The NOx emissions from soils display a zigzag distribution along latitude, largely because the croplands are distributed widely in both tropical and temperate regions.

[23] Figure 3 illustrates the global isoprene distributions during winter (December to February) and summer (June to August) of the Northern Hemisphere. Since isoprene emissions increase with temperature, light intensity, and foliar density, emissions are much higher during summer and at lower latitudes. It can be seen that isoprene emissions during winter months are concentrated in South America, central Africa, Southeast Asia, and northern Australia. The emission rate is normally more than 1500 mg C m^{-2} $month^{-1}$ in those regions, with the highest emission rate at about 4000 mg C m^{-2} $month^{-1}$. Very few emissions (less than 10 mg C m^{-2} $month^{-1}$) occur in the majority of areas beyond the midlatitude (30°N) of the Northern Hemisphere. On the other hand, in summer, large isoprene emissions (more than 2000 mg C m^{-2} $month^{-1}$) are found in the southeastern US, southern California, and southern China. In the Southern Hemisphere, only tropical South America and Africa emit large amounts of isoprene during the summer. The distinct seasonal fluctuations are found in temperate regions on both hemispheres. Overall, our model estimated global pattern of biogenic emissions are consistent with other studies [*Guenther et al.*, 1995; *Levis et al.*, 2003]. In terms of certain regional maximum emissions, our model estimates high summer emissions in eastern and western half of the United States, which are in agreement with *Guenther et al.* [2000]. In terms of absolute values, our model estimates, for example, summer

Table 3. Soil NOx Emissions by Region in 2000[a]

Region	Fertilizer-Induced Emissions	Total Cropland Emissions	Total Emissions
North America	0.311	0.387	0.576
Latin America	0.136	0.165	1.688
Europe	0.302	0.367	0.417
NAME[b]	0.102	0.125	0.297
Tropical Africa	0.034	0.234	1.589
Former Soviet Union	0.064	0.162	0.313
China	0.605	0.684	0.836
S and SE Asia	0.464	0.799	1.208
PDR[c]	0.061	0.084	0.585

[a]Emissions are in Tg N.
[b]NAME, North Africa and Middle East.
[c]PDR, Pacific Developed Regions.

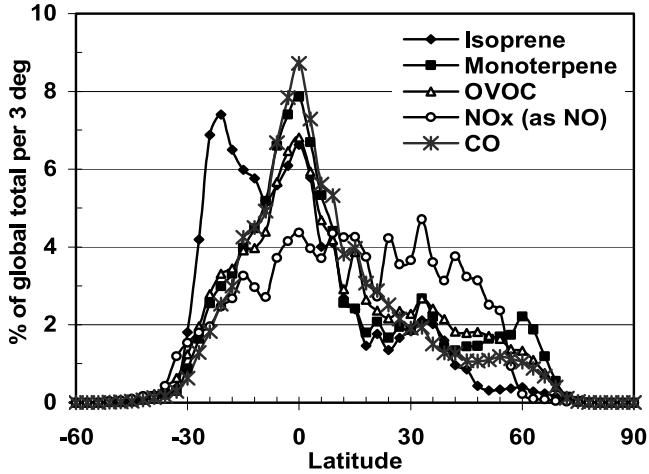

Figure 2. Model estimated zonal averaged biogenic emissions of the indirect GHGs (% of global total per 3°) for the year 2000.

monthly isoprene emission rates for the North America ranges from 0 to over 2000 mg C m^{-2} $month^{-1}$ (Figure 3), consistent with *Guenther et al.* [2000] estimates.

[24] Since the distributions of all other carbon containing gases (i.e., monoterpene, OVOC, and CO) are about the same, we take monoterpene as an example to discuss the global distributions of biogenic emissions of other gases. Figure 4 shows the global map of monoterpene emissions during winter and summer. Similar to isoprene distributions, monoterpene emissions display large seasonal variation in temperate and boreal regions, particularly between 50°N and 70°N, and there are almost no monthly variations along the equator.

[25] Figure 5 illustrates the winter and summer NOx emissions from soils with the *CRF*. NOx emissions display distinct seasonality in both hemispheres. NOx emissions in summer are significantly higher than in winter for the Northern Hemisphere. As expected, the seasonal trend is opposite in the Southern Hemisphere. Temperature, pulsing effects, and fertilizer usage contribute to this seasonal variation in global biogenic NOx emission. In tropical regions the seasonal distinction largely results from the pulsing effect because temperature and fertilizer usage are quite uniform throughout the year. In extratropical regions high temperature and fertilizer usage lead to maximum emissions during growing summer season. Croplands are the largest emitters of NOx, and are heavily impacted by human usage of nitrogen-containing fertilizers, particularly in central North America, India, large potions of Europe and Russia, eastern China, and Southeast Asia (Table 3). The NOx emission rates from croplands are generally greater than 20 mg N m^{-2} $month^{-1}$ during summer months.

[26] It is important to note that the application of the *CRF* has a large impact on estimations of NOx emissions from soils. Estimated NOx emissions are systematically lower with the *CRF* than without the *CRF*, particularly in the tropical forest areas (i.e., the Amazon, central Africa, and Southeast Asia). Our model estimated *CRF* effect in tropical forests lies in the approximate range of 50–70% (Table 2) as compared to *Ganzeveld et al.* [2002] estimates of 40%–50% reduction based on their model study. According to recent LAB-EUSTACH measurements at an Amazonian rain forest site [*Andreae et al.*, 2002; *Gut et al.*, 2002a, 2002b; *Pinto et al.*, 2002; *Rummel et al.*, 2002], *Gut et al.* [2002b] reported about 74% reduction of NOx emissions at night due to deposition onto forest soils and 34% during daytime. It should be noted that *Gut et al.*'s [2002b] figures did not include the effect of leaf uptake of NO_2. Nevertheless, significant changes in natural NOx emissions from different biomes, as we have noticed in our calculations for with and without the *CRF*, can have a large impact on global tropospheric chemistry, particularly on tropospheric O_3 and CH_4 chemistry, and thus can impose a significant impact on climate.

3.2. Model Intercomparison

[27] There are a number of modeling studies of biogenic emissions on both global and regional scales with which to

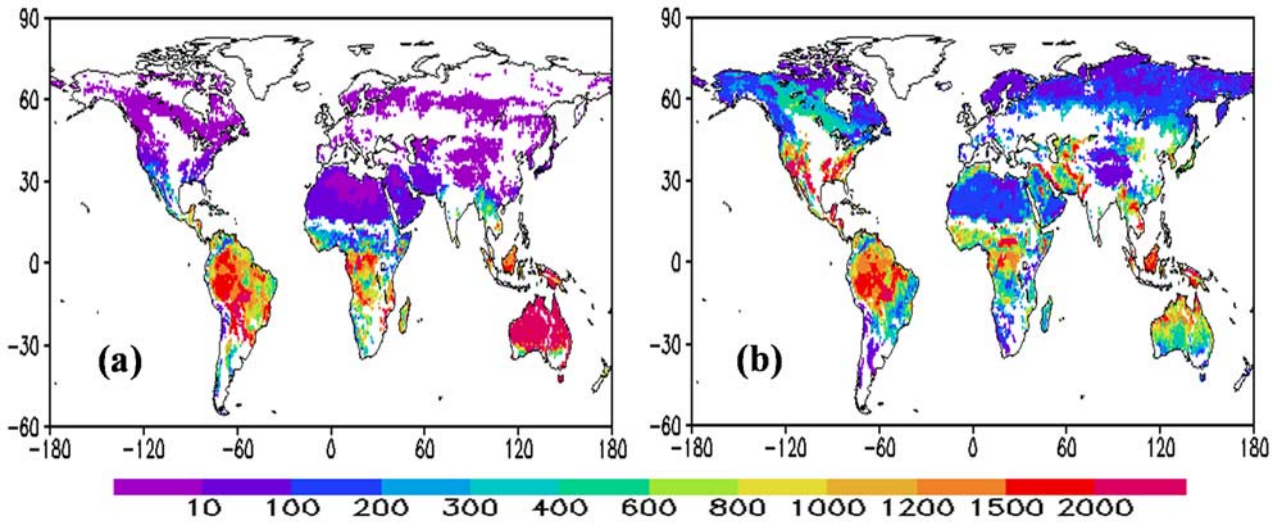

Figure 3. Model estimated global distributions of vegetation isoprene emissions (mg C m^{-2} $month^{-1}$) for year 2000 (a) winter and (b) summer of the Northern Hemisphere.

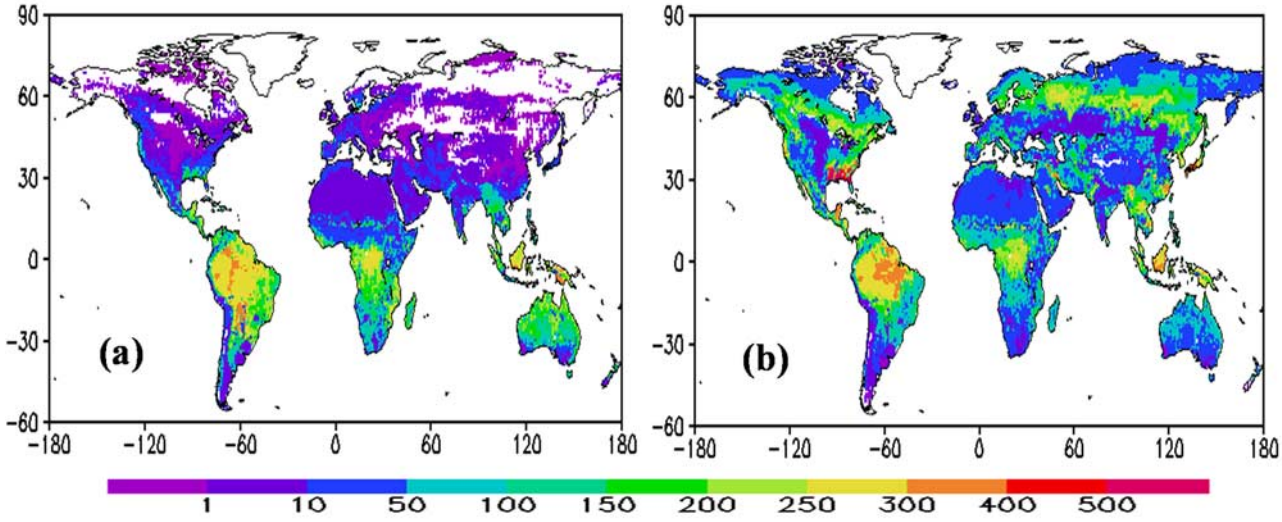

Figure 4. Model estimated global distributions of vegetation monoterpene emissions (mg C m^{-2} $month^{-1}$) for year 2000 (a) winter and (b) summer of the Northern Hemisphere.

evaluate our model results. On a global scale, ISAM estimated annual isoprene emissions of 601 Tg C are similar to *Guenther et al.* [1995], *Wang and Shallcross* [2000], *Adams et al.* [2001], *Potter et al.* [2001], *Levis et al.* [2003], and *Naik et al.* [2004] (Table 4). The isoprene emissions from *Muller* [1992] are about 50% lower than what we modeled, probably because the two studies use different algorithms, different input data, and different emission factors (ε) to calculate the isoprene emissions. For example, we employed the algorithm of *Guenther et al.* [1995], whereas *Muller* [1992] used a parameterization scheme employing temperature-dependent hydrocarbon emission algorithms developed by *Lamb et al.* [1987] and *NPP* calculated according to the empirical relationships adopted in the Miami model [*Leith*, 1975]. Our isoprene estimation is also significantly higher than what is given by the *IPCC* [2001]. This may be because the IPCC estimates are based on an inverse method using a global chemical transport model (CTM). The IPCC, however, cautions that incomplete knowledge of vegetation canopy reduction and surface uptake might lead to the mismatch of the CTM modeled and observed isoprene concentrations. Although there is some evidence for microbial consumption of isoprene in temperate forest soils [*Cleveland and Yavitt*, 1998], the data are insufficient at present to include in global inventories. The large discrepancy between this study and that of the IPCC only indicates that more work needs to be carried out to reduce the uncertainty in estimates of biogenic isoprene emissions.

[28] The global monoterpene emissions from our model (103 Tg C) fall within the range (33–147 Tg C) of the studies listed in Table 4. The apparent difference chiefly arises from the selection of ε and foliar density. Meteorology also plays an important role in accounting for these

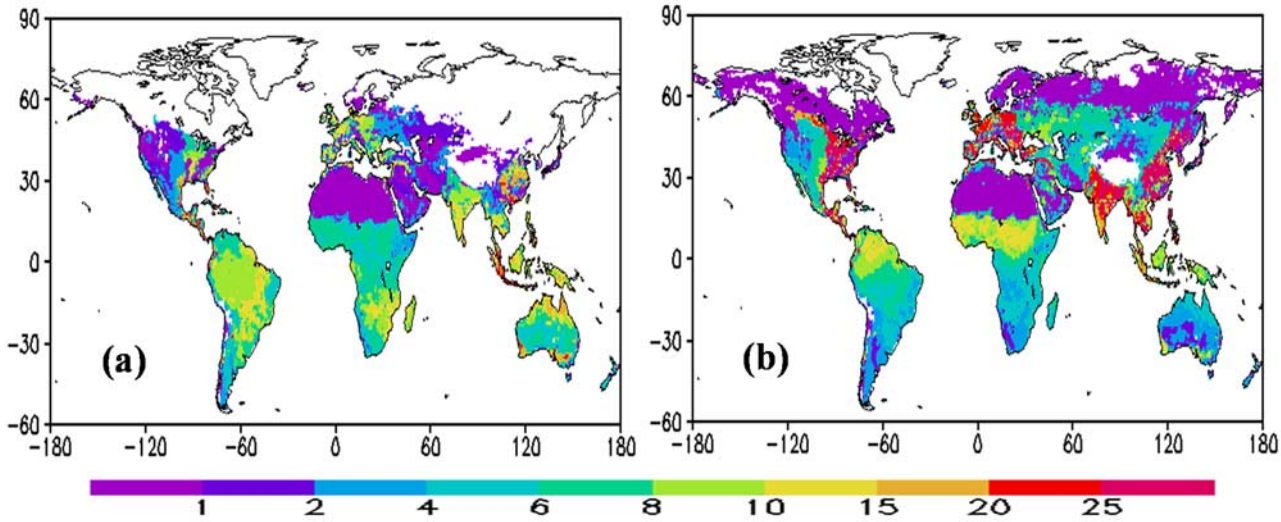

Figure 5. Model estimated global distributions of soil NOx emissions (mg N m^{-2} $month^{-1}$) for year 2000 (a) winter and (b) summer of the Northern Hemisphere.

Table 4. Comparison of Biogenic Emissions of Indirect GHGs to Other Studies[a]

Sources	Isoprene	Monoterpene	NOx
Global			
This study	601	103	7.51
Muller [1992]	250	147	6.7
Guenther et al. [1995]	503	127	
Yienger and Levy [1995]			5.45
Potter et al. [1996]			9.69
Davidson and Kingerlee [1997]			21
Lee et al. [1997]			7.0
Wang and Shallcross [2000]	530		
Adams et al. [2001]	561	117	
Food and Agricultural Organization [2001]			13.4
IPCC [2001]	220	127	5.6
Potter et al. [2001]	559		
Ganzeveld et al. [2002]			12
Levis et al. [2003]	507	33	
Naik et al. [2004]	454	72	
Europe			
This study	1.17	1.73	0.417
Simpson et al. [1995][b]	1.95		0.436
Stohl et al. [1996][c]			0.415
North America			
This study	29.4	8.90	0.576
Guenther et al. [2000]	29.3	17.9	0.9
Africa South of the Equator			
This study	52.3	10.8	0.687
Guenther et al. [1995]	59	11.8	
Otter et al. [2003]	56	7.2	
African EXPRESSO Domain			
This study	47.8	8.77	0.392
Guenther et al. [1995]	41.1		
Guenther et al. [1999]	35.4		
Contiguous USA			
This study	23.2	4.87	0.491
Williams et al. [1992]			0.314
Yienger and Levy [1995]			0.37
Guenther et al. [1995]	24	8	
Guenther et al. [2000]	15.5	7.52	0.441
United Kingdom			
This study	0.012	0.0218	0.0270
Simpson et al. [1995][d]	0.0227		0.0229
Stohl et al. [1996]			0.0254
Simpson et al. [1999]	0.0577	0.0312	
Stewart et al. [2003]	0.008	0.083	

[a]Unit for NOx is Tg N yr^{-1}; unit for other species is Tg C yr^{-1}.
[b]Exclude the European part of former USSR. Take E-94 isoprene emissions.
[c]Exclude former USSR.
[d]Take E-94 isoprene emissions.

discrepancies. Our estimation of global and annual soil emissions of NOx with the *CRF* effects is 7.51 Tg N, which compares well with the lower range of values (5.45–21 Tg N) estimated by other studies (Table 4). *Yienger and Levy* [1995] and *Lee et al.* [1997] also included the *CRF* to estimate NOx emissions from soils. *Davidson and Kingerlee* [1997], however, questioned whether the *CRF* should be applied systematically to all the biomes since many field measurements were made above the canopies. With this debate in mind, we also calculated NOx emissions from soils without using the *CRF*. The resultant annual NOx emissions from soils increase to 15.42 Tg N, doubling the value with the *CRF*. Therefore our estimated value of 7.51 Tg N should be regarded as a lower bound for annual global NOx emissions from soils.

[29] On a regional scale, our model estimated biogenic emissions of the indirect GHGs fall within ±50% of other available estimates. There are few exceptions where the differences are more than 100%. The discrepancy may stem from the different biome classifications, differences in the regional areas and boundaries, different emission factors assigned to each grid, and the different meteorological conditions applied in each study.

3.3. Historical Vegetation Emissions for the Period 1981–2000

[30] Figure 6 shows the global mean monthly variations in isoprene emissions over the period 1981–2000 for the *E1* case. Figure 6 suggests that monthly simulated emissions vary as much as 31% from year to year because of combined effects of land cover changes, atmospheric CO_2 increases, and climate variations. Our model estimated monthly variations are about 6–12% higher than the other recent modeling studies [*Levis et al.*, 2003; *Naik et al.*, 2004]. The yearly variations (not shown here) are much smaller than the monthly variations.

[31] The monthly variations in emissions (Figure 6) are mainly due to the monthly absolute temperature variations. The monthly temperature effect can be further illustrated by comparing monthly mean isoprene emissions (Figure 7) over the period 1981–2000 for three major foliage emitters, i.e., tropical forests, savanna, and boreal forests. Higher temperatures in tropical forests and savannas result in the higher isoprene emissions, whereas the reverse is true in the case of boreal forests. The emissions from boreal forests and savanna show a clear seasonal pattern with maximum emissions during their summer months, whereas emissions from tropical forests have small seasonal variations because the plant productivity is high throughout the year in humid tropical regions. It is also interesting to note that, during the

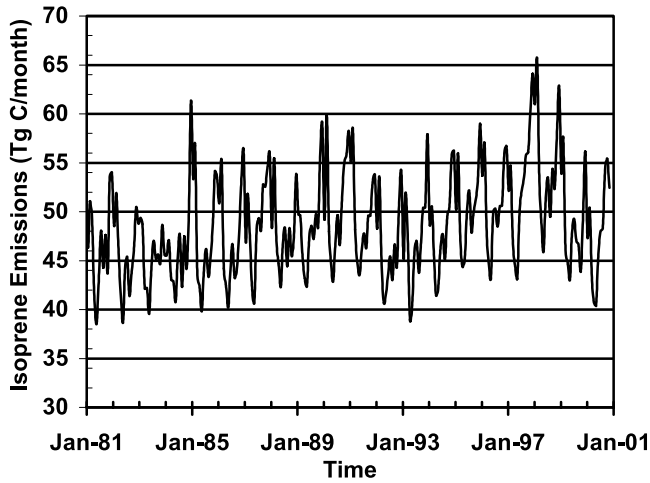

Figure 6. Model estimated global and monthly mean vegetation isoprene emissions over the period 1981–2000 based on *E1* experiment, in which land cover changes, atmospheric CO_2, and climate change were varied over the historical time period.

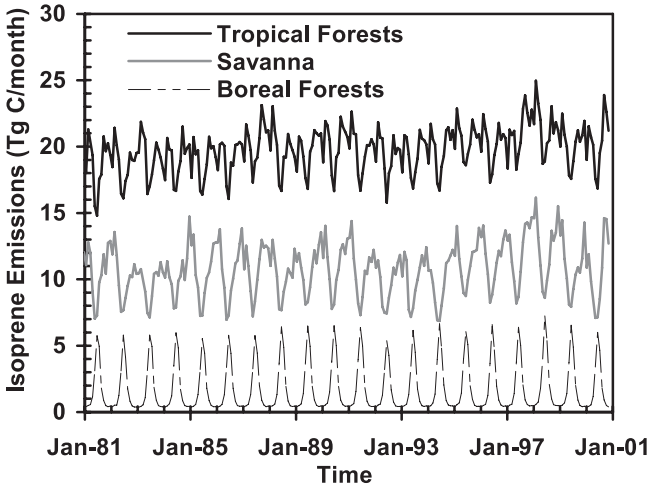

Figure 7. Model estimated monthly mean isoprene emissions from tropical forests, savanna, and boreal forests over the period 1981–2000.

past 20 years from 1981 to 2000, the highest emissions occur in the year 1998. It should be noted that 1998 was a strong El Niño year characterized by warmer and drier conditions in tropical areas, which, in turn, favors higher biogenic emissions. The coincidence of higher vegetation emissions and an El Niño event is evident from this case study. However, the quantitative relationship needs to be established through long-term observations in the tropics.

[32] The effect of land cover change, climate change, and atmospheric CO_2 increase over the period 1981–2000 can be quantified by analyzing the annual variation rate of isoprene emissions. As Figure 8 shows, over the period 1981–1992, on average around 2%/yr (11 Tg C/yr) less vegetation emissions of isoprene have occurred because of land cover change. It is mainly because, over the 20 years, natural land ecosystems are cleared for croplands; and as discussed in section 3.1, croplands are negligible isoprene emitters compared to other natural ecosystems. Prior to 1981, there could have been much larger NMVOC emissions reductions due to land cover change activities, because historical data of land cover change for croplands show a generally increasing rate of change of activities until 1960. Thereafter, the data reveal decreasing land cover change activities until 1992 [*Ramankutty and Foley*, 1998].

[33] Figure 8 also illustrates that with changing climate, yearly isoprene emissions over the period 1981–2000 vary between −8 and 56 Tg C as compared to constant climate conditions. There are large annual emission variations due to climate change. Nevertheless emissions show an upward trend as a result of global mean temperature increase over the past 2 decades. Averaging 1981–2000, approximately 2%/yr (12 Tg C/yr) more isoprene emissions occur with changing climate as compared to constant climate.

[34] The emissions also vary in response to changes in atmospheric CO_2 increases. As a result of atmospheric CO_2 increases, the model estimated overall *NPP* increase over the period 1981–2000 is about 3 Gt C, mainly because of the CO_2 fertilization effect. The increased *NPP* yields heavier foliage mass and woody vegetation that generates more emissions of isoprene and other NMVOCs [*Guenther et al.*, 1994; *Kesselmeier and Staudt*, 1999; *Fuentes et al.*, 2000, 2001; *Shallcross and Monks*, 2000]. On the basis of our model results, isoprene emissions on the basis of a 20 year average are predicted to increase by 9%/yr (53Tg C/yr) over the period 1981–2000 (Figure 8).

[35] These results suggest that the changes in land cover and climate, and increasing atmospheric CO_2 could have a significant effect on the biogenic NMVOCs emissions. Therefore it is important to account for these effects not only for the historical NMVOCs emissions simulations, but also for future emission scenarios for the biogenic emissions.

4. Conclusions and Future Research

[36] As one of the crucial steps to expand the capability of ISAM, a global biogenic emission model has been coupled to the terrestrial ecosystem component of the ISAM to study the biogenic emissions of indirect GHGs. This coupling provides a unique capability to investigate the time-dependent changes in biogenic emissions due to changes in ecological and physiological processes and their interactions with atmospheric CO_2, climate, and human-induced land cover changes. The modeled vegetation emissions are about 601 Tg C/yr for isoprene, 103 Tg C/yr for monoterpene, 102 Tg C/yr for OVOC, and 73 Tg C/yr for CO. Soil emissions of NOx are estimated at 7.51 Tg N/yr. Compared to other recent modeling studies, our results for the global case generally are consistent. However, on the regional scale, there is a substantial difference between our model results and other available estimates. In some cases the difference is more than 100%, largely because of differences in biome classifications, and differences in assigned emission factors. Vegetation emissions of isoprene and OVOC respond to changes in land cover, increase in CO_2 concentrations, and climate variations. Large-scale conversions of natural biomes, e.g., tropical forests into croplands, lead to the declining trend of emissions. On average, an approximate 2%/yr decrease in isoprene and

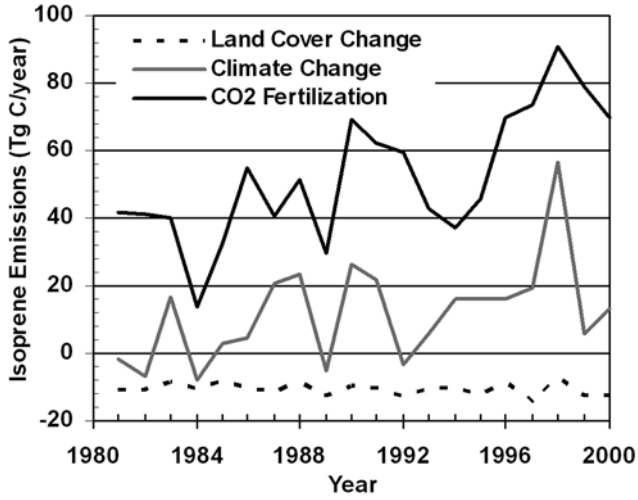

Figure 8. Model estimated effect of land cover change, climate change, and atmospheric CO_2 increase on the global and annual mean vegetation isoprene emissions over the period 1981–2000.

OVOC emissions is seen compared to the scenario with no land cover change since 1765. Increased CO_2 concentrations increase foliage mass as a result of CO_2 fertilization feedback in the model. This results in greater emissions of isoprene and OVOC. Model results show large seasonal variations in isoprene emissions from savanna and boreal forests, whereas tropical forests with high productivity throughout the year show small seasonal variations. Moreover, the model-simulated results suggest that the biogenic emissions of NMVOCs under the global warming scenario are expected to increase.

[37] On an annual basis and by average, CO_2 increase and climate change are responsible for 53 Tg C/yr and 12 Tg C/yr increase in isoprene emissions from 1981 to 2000, respectively, while land use changes cause a 11 Tg C/yr decline of isoprene emissions. The CO_2 increase is also the largest contributor to monoterpene changes from 1981 to 2000, followed by climate effect and land cover changes.

[38] The global and regional estimates of biogenic emissions of indirect GHGs presented in this study are designed to be used as inputs to socioeconomics models to develop future emission scenarios, and inputs to atmospheric chemistry models for tropospheric chemistry studies on GHGs, particularly on CH_4 and tropospheric O_3. A fully coupled ISAM could potentially provide an internally consistent framework to investigate the impact of climate change on emissions, chemistry, and ecosystems, as well as feedbacks of changing emissions and chemistry to future climate. The biogenic emissions results will be updated with time and made available on the ISAM web site (http://isam.atmos.uiuc.edu/).

[39] **Acknowledgments.** We thank Alex Guenther for providing valuable comments on the earlier version of this manuscript as well as for the grid-based emission factors used in this study. We also thank Xiaojuan Yang for assistance with ISAM terrestrial model calculations. This research was supported in part by the Office of Science (BER), U.S. Department of Energy (DOE-DE-FG02-01ER63463).

References

Adams, J. M., J. V. H. Constable, A. Guenther, and P. Zimmerman (2001), An estimate of natural volatile organic compounds emissions from vegetation since the last glacial maximum, *Chemosphere*, *3*, 73–91.

Andreae, M. O., et al. (2002), Biogeochemical cycling of carbon, water, energy, trace gases, and aerosols in Amazonia: The LBA-EUSTACH experiments, *J. Geophys. Res.*, *107*(D20), 8066, doi:10.1029/2001JD000524.

Bertin, N., M. Staudt, U. Hansen, G. Seufert, P. Ciccioli, P. Foster, J. L. Fugit, and T. Torres (1997), Diurnal and seasonal course of monoterpene emissions from *Quercus Ilex* (L.) under natural conditions—Application of light and temperature algorithms, *Atmos. Environ.*, *31*, 135–144.

Bonan, G. B., K. W. Olson, M. Vertenstin, S. Levis, X. Zeng, Y. Dai, R. E. Dickinson, and Z.-L. Yang (2002), The land surface climatology of the Community Land Model coupled to the NCAR Community Climate Model, *J. Clim.*, *15*, 3123–3149.

Ciccioli, P., C. Fabozzi, E. Brancaleoni, A. Cecinato, M. Frattoni, S. Cieslik, D. Kotzias, G. Seufert, P. Foster, and R. Steinbrecher (1997), Biogenic emission from the Mediterranean pseudosteppe ecosystem present in Castelporziano, *Atmos. Environ.*, *31*, 167–175.

Cleveland, C. C., and J. B. Yavitt (1998), Microbial consumption of atmospheric isoprene in a temperate forest soil, *Appl. Environ. Microbiol.*, *64*, 172–177.

Cramer, W., et al. (1999), Comparing global models of terrestrial net primary productivity (NPP): Overview and key results, *Global Change Biol.*, *5*, 1–15.

Daniel, J. S., and S. Solomon (1998), On the climate forcing of carbon monoxide, *J. Geophys. Res.*, *103*, 13,249–13,260.

Davidson, E. A., and W. Kingerlee (1997), A global inventory of nitric oxide emissions from soils, *Nutrient Cycling Agroecosyst.*, *48*, 37–50.

Fall, R. (1999), Biogenic emissions of volatile organic compounds from higher plants, in *Reactive Hydrocarbons in the Atmosphere*, edited by C. N. Hewitt, pp. 41–94, Elsevier, New York.

Foley, J. A., I. C. Prentice, N. Ramankutty, S. Levis, D. Pollard, S. Stich, and A. Haxeltine (1996), An integrated model of land surface processes, terrestrial carbon balance, and vegetation dynamics, *Global Biogeochem. Cycles*, *10*, 603–628.

Food and Agricultural Organization (2001), *Global Estimates of Gaseous Emissions of NH_3, NO and N_2O From Agricultural Land*, Food and Agric. Organ. of the U. N., Rome.

Friedli, H., H. Lotscher, H. Oeschger, U. Siegenthaler, and B. Stauffer (1986), Ice core record of 13C/12C ratio of atmospheric CO_2 in the past two centuries, *Nature*, *324*, 237–238.

Fuentes, J. D., et al. (2000), Biogenic hydrocarbons in the atmospheric boundary layer: A review, *Bull. Am. Meteorol. Soc.*, *81*, 1537–1575.

Fuentes, J. D., B. P. Hayden, M. Garstang, M. Lerdau, D. Fitzjarrald, D. D. Baldocchi, R. Monson, B. Lamb, and C. Geron (2001), VOCs and biosphere-atmosphere feedbacks, *Atmos. Environ.*, *31*, 189–191.

Fuglestvedt, J. S., I. S. A. Isaksen, and W.-C. Wang (1996), Estimates of indirect global warming potentials for CH_4, CO, and NOx, *Clim. Change*, *34*, 405–437.

Galbally, I. E., and C. R. Roy (1978), Loss of fixed nitrogen from soils by nitric oxide exhalation, *Nature*, *275*, 734–735.

Ganzeveld, L. N., J. Lelieveld, F. J. Dentener, M. C. Krol, A. J. Bouwman, and G. J. Roelofs (2002), Global soil-biogenic NOx emissions and the role of canopy processes, *J. Geophys. Res.*, *107*(D16), 4298, doi:10.1029/2001JD001289.

Geron, C., A. Guenther, and T. Pierce (1994), An improved model for estimating emissions of volatile organic compounds from forests in the eastern United States, *J. Geophys. Res.*, *99*, 12,773–12,791.

Geron, C., D. Nie, R. R. Arnts, T. D. Sharkey, E. L. Singsaas, P. J. Vanderveer, A. Guenther, J. E. Sickles II, and T. E. Kleindienst (1997), Biogenic isoprene emission: Model evaluation in a southeastern United States bottomland deciduous forest, *J. Geophys. Res.*, *102*, 18,889–18,901.

Geron, C., A. Guenther, J. Greenberg, H. W. Loescher, D. Clark, and B. Baker (2002), Biogenic volatile organic compound emissions from a lowland tropical wet forest in Costa Rica, *Atmos. Environ.*, *36*, 3793–3802.

Greenberg, J. P., A. Guenther, S. Madronich, W. Baugh, P. Ginoux, A. Druilhet, R. Delmas, and C. Delon (1999), Biogenic volatile organic compound emissions in central Arica during the Experiment for the Regional Sources and Sinks of Oxidants (EXPRESSO) biomass burning season, *J. Geophys. Res.*, *104*, 30,659–30,671.

Guenther, A. (2002), The contribution of reactive carbon emissions from vegetation to the carbon balance of terrestrial ecosystems, *Chemosphere*, *49*, 837–844.

Guenther, A., P. Zimmerman, P. Harley, R. Monson, and R. Fall (1993), Isoprene and monoterpene emission rate variability: Model evaluation and sensitivity analysis, *J. Geophys. Res.*, *98*, 12,609–12,617.

Guenther, A., P. Zimmermann, and M. Wildermuth (1994), Natural volatile organic compound emission rate estimates for U.S. woodland landscapes, *Atmos. Environ.*, *28*, 1197–1210.

Guenther, A., et al. (1995), A global model of natural volatile organic compound emissions, *J. Geophys. Res.*, *100*, 8873–8892.

Guenther, A., L. Otter, P. Zimmerman, J. Greenberg, R. Scholes, and M. Scholes (1996a), Biogenic hydrocarbon emissions from southern African savannas, *J. Geophys. Res.*, *101*, 25,859–25,865.

Guenther, A., P. Zimmerman, L. Klinger, J. Greenberg, C. Ennis, K. Davis, W. Pollock, H. Westberg, G. Allwine, and C. Geron (1996b), Estimates of regional natural volatile organic compound fluxes from enclosure and ambient measurements, *J. Geophys. Res.*, *101*, 1345–1359.

Guenther, A., B. Baugh, G. Brasseur, J. Greenberg, P. Harley, L. Klinger, D. Serca, and L. Vierling (1999), Isoprene emission estimates and uncertainties for the central African EXPRESSO study domain, *J. Geophys. Res.*, *104*, 30,625–30,639.

Guenther, A., C. Geron, T. Pierce, B. Lamb, P. Harley, and R. Fall (2000), Natural emissions of non-methane volatile organic compounds, carbon monoxide, and oxides of nitrogen from North America, *Atmos. Environ.*, *34*, 2205–2230.

Gut, A., S. M. van Dijk, M. Scheibe, U. Rummel, M. Welling, C. Ammann, F. X. Meixner, G. A. Kirkman, M. O. Andreae, and B. E. Lehmann (2002a), NO emissions from an Amazonian rain forest soil: Continuous measurements of NO flux and soil concentration, *J. Geophys. Res.*, *107*(D20), 8057, doi:10.1029/2001JD000521.

Gut, A., et al. (2002b), Exchange fluxes of NO_2 and O_3 at soil and leaf surfaces in an Amazonian rain forest, *J. Geophys. Res.*, *107*(D20), 8060, doi:10.1029/2001JD000654.

Hakola, H., J. Rinne, and T. Laurila (1998), The hydrocarbon emission rates of Tea-leafed willow (Salix phylicifolia), silver birch (Betula pen-

dula) and European aspen (Populus tremula), *Atmos. Environ.*, *32*, 1825–1833.

Harley, P., L. Otter, A. Guenther, and J. Greenberg (2003), Micrometeorological and leaf-level measurements of isoprene emissions from a southern African savanna, *J. Geophys. Res.*, *108*(D13), 8468, doi:10.1029/2002JD002592.

Haxeltine, A., and I. C. Prentice (1996), BIOME3: An equilibrium terrestrial biosphere model based on ecophysiological constraints, resource availability, and competition among plant functional types, *Global Biogeochem. Cycles*, *10*, 693–709.

Hayhoe, K., A. Jain, H. S. Kheshgi, and D. Wuebbles (2000), Contribution of CH_4 to multi-gas reduction targets: The impact of atmospheric chemistry on GWPs, in *Non-CO_2 Greenhouse Gases: Scientific Understanding, Control and Implementation*, edited by J. van Ham, pp. 425–432, Springer, New York.

Heikes, B. G., et al. (2003), Atmospheric methanol budget and ocean implications, *Global Biogeochem. Cycles*, *16*(4), 1133, doi:10.1029/2002GB001895.

Helmig, D., L. F. Klinger, A. Guenther, L. Vierling, C. Geron, and P. Zimmerman (1999), Biogenic volatile organic compound emissions (BVOCs) II. Landscape flux potentials from three continental sites in the U.S., *Chemosphere*, *38*, 2189–2204.

Houyoux, M. R., J. M. Vukovich, C. J. Coats Jr., and N. J. M. Wheeler (2000), Emission inventory development and processing for the seasonal model for regional air quality (SMRAQ) project, *J. Geophys. Res.*, *105*, 9079–9090.

Intergovernmental Panel on Climate Change (2001), *Climate Change 2001: The Scientific Basis—Contribution of Working Group I to the Third Assessment Report of the Intergovernmental Panel on Climate Change*, edited by J. T. Houghton et al., 881 pp., Cambridge Univ. Press, New York.

International Fertilizer Industry Association (2005), *Nitrogen-Phosphate-Potash, IFADATA Statistics From 1973–1973/74 to 2002–2002/2003, Including Separate World Fertilizer Consumption Statistics*, Paris. (Available at http://www.fertilizer.org)

Jacob, D. J., and P. Bakwin (1991), Cycling of NOx in tropical forest canopies, in *Microbial Production and Consumption of Greenhouse Gases*, edited by J. Rogers and W. Whitman, pp. 237–253, Am. Soc. for Microbiol., Washington, D. C.

Jain, A. K., and X. Yang (2005), Modeling the effects of two different land cover change data sets on the carbon stocks of plants and soils in concert with CO_2 and climate change, *Global Biogeochem. Cycles*, *19*, GB2015, doi:10.1029/2004GB002349.

Janson, R. W. (1993), Monoterpene emissions from Scots pine and Norwegian spruce, *J. Geophys. Res.*, *98*, 2839–2850.

Keeling, C. D., and T. P. Whorf (2000), Atmospheric CO_2 records from sites in the SIO air sampling network, in *Trends: A Compendium of Data on Global Change*, Carbon Dioxide Inf. Anal. Cent., Oak Ridge Natl. Lab., Oak Ridge, Tenn. (Available at http://cdiac.esd.ornl.gov/trends/co2/sio-mlo.htm)

Kesselmeier, J., and M. Staudt (1999), Biogenic volatile compounds (VOC): An overview on emission, physiology and ecology, *J. Atmos. Chem.*, *33*, 23–88.

Kheshgi, H. S., and A. K. Jain (1999), Reduction of the atmospheric concentration of methane as a strategic response option to global climate change, in *Greenhouse Gas Control Technologies*, edited by P. Reimer, B. Eliasson, and A. Wakaun, pp. 775–780, Elsevier, New York.

Kheshgi, H. S., A. K. Jain, R. Kotamarthi, and D. J. Wuebbles (1999), Future atmospheric methane concentrations in the context of the stabilization of greenhouse gas concentrations, *J. Geophys. Res.*, *104*, 19,183–19,190.

Lamb, B., A. Guenther, D. Gay, and H. Westberg (1987), A national inventory of biogenic hydrocarbon emissions, *Atmos. Environ.*, *21*, 1695–1705.

Lee, D. S., I. Kohler, E. Grobler, F. Rohrer, R. Sausen, L. Gallardo-Klenner, J. G. J. Olivier, F. J. Dentener, and A. F. Bouwman (1997), Estimations of global NOx emissions and their uncertainties, *Atmos. Environ.*, *31*, 1735–1749.

Leith, H. (1975), Modeling the primary productivity of the world, in *Primary Productivity of the Biosphere*, edited by H. Leith and R. H. Whittaker, pp. 237–263, Springer, New York.

Levis, S., C. Wiedinmyer, G. B. Bonan, and A. Guenther (2003), Simulating biogenic volatile organic compound emissions in the Community Climate System Model, *J. Geophys. Res.*, *108*(D21), 4659, doi:10.1029/2002JD003203.

Li, Z., and H. G. Leighton (1993), Global climatology of the solar radiation budgets at the surface and in the atmosphere from 5 years of ERBE data, *J. Geophys. Res.*, *98*, 4919–4930.

Li, Z., H. G. Leighton, K. Masuda, and T. Takashima (1993), Estimation of SW flux absorbed at the surface from TOA reflected flux, *J. Clim.*, *6*, 317–330.

Loveland, T. R., and A. S. Belward (1997), The IGBP-DIS global 1 km land cover data set, DISCover: First results, *Int. J. Remote Sens.*, *18*, 3291–3295.

Muller, J.-F. (1992), Geographical distribution and seasonal variation of surface emissions and deposition velocities of atmospheric trace gases, *J. Geophys. Res.*, *97*, 3787–3804.

Myneni, R. B., R. R. Nemani, and S. W. Running (1997), Estimation of global leaf area index and absorbed PAR using radiative transfer models, *IEEE Trans. Geosci. Remote Sens.*, *35*, 1380–1393.

Naik, V., C. Delire, and D. J. Wuebbles (2004), Sensitivity of global biogenic isoprenoid emissions to climate variability and atmospheric CO_2, *J. Geophys. Res.*, *109*, D06301, doi:10.1029/2003JD004236.

Neftel, A., E. Moor, H. Oeschger, and B. Stauffer (1985), Evidence from polar ice cores for the increase in atmospheric CO_2 in the past two centuries, *Nature*, *315*, 45–47.

Otter, L., A. Guenther, C. Wiedinmyer, G. Fleming, P. Harley, and J. Greenberg (2003), Spatial and temporal variations in biogenic volatile organic compound emissions from Africa south of equator, *J. Geophys. Res.*, *108*(D13), 8505, doi:10.1029/2002JD002609.

Owen, S. M., P. Harley, A. Guenther, and C. N. Hewitt (2002), Light dependence of VOC emissions from selected Mediterranean plant species, *Atmos. Environ.*, *36*, 3147–3159.

Pastor, J., and W. M. Post (1985), Development of a linked forest productivity-soil process model, *Tech. Rep. ORNL/TM-9519*, Oak Ridge Natl. Lab., Oak Ridge, Tenn.

Pattey, E., R. L. Desjardins, H. Westberg, B. Lamb, and T. Zhu (1999), Measurement of isoprene emissions over a black spruce stand using a tower-based relaxed eddy-accumulation system, *J. Appl. Meteorol.*, *38*, 870–877.

Pierce, T., C. Geron, L. Bender, R. Dennis, G. Tonnesen, and A. Guenther (1998), Influence of increased isoprene emissions on regional ozone modeling, *J. Geophys. Res.*, *103*, 25,611–25,629.

Pinto, A. S., M. M. C. Bustamante, K. Kisselle, R. Burke, R. Zepp, L. T. Viana, R. F. Varella, and M. Molina (2002), Soil emissions of N_2O, NO, and CO_2 in Brazilian savanna: Effects of vegetation type, seasonality, and prescribed fires, *J. Geophys. Res.*, *107*(D20), 8089, doi:10.1029/2001JD000342.

Potter, C. S., P. A. Matson, P. M. Vitousek, and E. A. Davidson (1996), Process modeling of controls on nitrogen trace gas emissions from soils worldwide, *J. Geophys. Res.*, *101*, 1361–1377.

Potter, C. S., S. E. Alexander, J. C. Coughlan, and S. A. Klooster (2001), Modeling biogenic emissions of isoprene: Exploration of model drivers, climate control algorithms, and use of global satellite observations, *Atmos. Environ.*, *35*, 6151–6165.

Potter, C., S. Klooster, D. Bubenheim, H. W. Sing, and R. Myneni (2003), Modeling terrestrial biogenic sources of oxygenated organic emissions, *Earth Interact.*, *7*, 1–7.

Prentice, C., G. Farquhar, M. Fasham, M. Goulden, M. Heimann, V. Jaramillo, H. Kheshgi, C. L. Quere, R. Scholes, and D. Wallace (2001), The carbon cycle and atmospheric CO_2, in *Climate Change 2001: The Scintific Basis—Contribution of WGI to the Third Assessment Report of the IPCC*, edited by J. T. Houghton et al., pp. 183–237, Cambridge Univ. Press, New York.

Purves, D. W., J. P. Caspersen, P. R. Moorcroft, G. C. Hurtt, and S. W. Pacala (2004), Human-induced changes in US biogenic volatile organic compound emissions: Evidence from long-term forest inventory data, *Global Change Biol.*, *10*, 1–19, doi:10.1111/j.1365-2486.2004.00844.x.

Ramankutty, N., and J. Foley (1998), Characterizing patterns of global land use: An analysis of global croplands data, *Global Biogeochem. Cycles*, *12*, 667–685.

Ramankutty, N., and J. A. Foley (1999), Estimating historical changes in global land cover: Croplands from 1700 to 1992, *Global Biogeochem. Cycles*, *13*, 997–1027.

Rawls, W. J., D. L. Brakensiek, and K. E. Saxton (1982), Estimation of soil water properties, *Trans. ASAE*, *25*, 1316–1328.

Rummel, U., C. Ammann, A. Gut, F. X. Meixner, and M. O. Andreae (2002), Eddy covariance measurements of nitric oxide flux within an Amazonian rain forest, *J. Geophys. Res.*, *107*(D20), 8050, doi:10.1029/2001JD000520.

Schade, G. W., and P. J. Crutzen (1999), CO emissions from degrading plant matter (II). Estimate of a global source strength, *Tellus, Ser. B*, *51*, 909–918.

Schade, G. W., R.-M. Hofmann, and P. J. Crutzen (1999), CO emissions from degrading plant matter (I). Measurements, *Tellus, Ser. B*, *51*, 889–908.

Shallcross, D. E., and P. S. Monks (2000), New directions: VOCs and biospherie-atmosphere feedbacks, *Atmos. Environ.*, *35*, 189–191.

Silver, G., and R. Fall (1995), Characterization of aspen isoprene syntheses, an enzyme responsible for leaf isoprene emission to the atmosphere, *J. Biol. Chem.*, *270*, 13,010–13,016.

Simpson, D., A. Guenther, C. N. Hewitt, and R. Steinbrecher (1995), Biogenic emissions in Europe: 1. Estimates and uncertainties, *J. Geophys. Res.*, *100*, 22,875–22,890.

Simpson, D., et al. (1999), Inventorying emissions from nature in Europe, *J. Geophys. Res.*, *104*, 8113–8152.

Steinbrecher, R., K. Hauff, R. Rabong, and J. Steinbrecher (1997), The BEMA-project: Isoprenoid emission of oak species typical for the Mediterranean area—Source strength and controlling variables, *Atmos. Environ.*, *31*, 79–88.

Stewart, H. E., C. N. Hewitt, R. G. H. Bunce, R. Steinbrecher, G. Smiatek, and T. Schoenemeyer (2003), A highly spatially and temporally resolved inventory for biogenic isoprene and monoterpene emissions: Model description and application to Great Britain, *J. Geophys. Res.*, *108*(D20), 4644, doi:10.1029/2002JD002694.

Stohl, A., E. Williams, G. Wotawa, and H. Kromp-Kolb (1996), A European inventory of soil nitric oxide emissions and the effect of these emissions on the photochemical formation of ozone, *Atmos. Environ.*, *30*, 3741–3755.

Tao, Z., S. Larson, D. J. Wuebbles, A. Williams, and M. Caughey (2003), A seasonal simulation of biogenic contributions to ground-level ozone over the continental United States, *J. Geophys. Res.*, *108*(D14), 4404, doi:10.1029/2002JD002945.

Tarr, M. A., W. L. Miller, and R. G. Zepp (1995), Direct carbon monoxide photo-production from plant matter, *J. Geophys. Res.*, *100*, 11,403–11,413.

Thornthwaite, C. W., and J. R. Mather (1957), Instructions and tables for computing potential evapotranspiration and the water balance, *Publ. Climatol.*, *10*, 183–311.

Wang, K.-Y., and D. E. Shallcross (2000), Modeling terrestrial biogenic isoprene fluxes and their potential impact on global chemical species using a coupled LSM-CTM model, *Atmos. Environ.*, *34*, 2909–2925.

Webb, R. S., C. E. Rosenzweig, and E. R. Levine (1991), A global data set of soil particle size properties, *NASA Tech. Memo. 4286*, NASA Goddard Inst. for Space Stud., New York.

Williams, E. J., A. Guenther, and F. C. Fehsenfeld (1992), An inventory of nitric oxide emissions from soils in the United States, *J. Geophys. Res.*, *97*, 7511–7519.

Yienger, J. J., and H. Levy II (1995), Empirical model of global soil-biogenic NOx emissions, *J. Geophys. Res.*, *100*, 11,447–11,464.

Zobler, L. (1986), A world soil file for global climate modeling, *NASA Tech. Memo. 87802*, NASA Goddard Inst. for Space Stud., New York.

Zobler, L. (1999), Global soil types, 1-degree grid (Zobler) data set, http://www.daac.ornl.gov, Oak Ridge Natl. Lab. Distrib. Active Arch. Cent., Oak Ridge, Tenn.

A. K. Jain and Z. Tao, Department of Atmospheric Science, University of Illinois, Urbana, IL 61801, USA. (jain@atmos.uiuc.edu)